Preliminary characterization of calcium chemical environment in apatitic and non-apatitic calcium phosphates of biological interest by X-ray absorption spectroscopy

D. Eichert, M. Salomé, M. Banu, J. Susini and C. Rey

European Synchrotron Facility, X-ray Microscopy Beamline ID21, BP 220, 38043 Grenoble Cedex, France
CIRIMAT — ENSIACET, 118, route de Narbonne, 31077 Toulouse Cedex, France

Abstract

Several reports have mentioned the existence of non-apatitic environments of phosphate and carbonate ions in synthetic and biological poorly crystalline apatites. However there were no direct spectroscopic evidences for the existence of non-apatitic environment of calcium ions. X-ray Absorption Spectroscopy, at the K-edge of calcium, allows the discrimination between different calcium phosphates of biological interest despite great spectral similarities. A primary analysis of the spectra reveals the existence, in synthetic poorly crystalline apatites, of variable features related to the maturation stage of the sample and corresponding to the existence of non-apatitic environments of calcium ions. Although these features can also be found in several other calcium phosphate salts, and do not allow a clear identification of the ionic environments of calcium ions, they give a possibility to directly determine the maturity of poorly crystalline apatite from calcium X-ray Absorption Near Edge Structure spectra.

Keywords: Calcium phosphate; XAS; Microspectroscopy; Maturation; Synchrotron

1. Introduction

Recent progresses in the investigation of the short-range ionic organization of Poorly Crystalline Apatitic calcium phosphates (PCA) have been made possible by the use of spectroscopic techniques such as Fourier Transform Infra Red (FTIR), Raman and Magic Angle Spinning – Nuclear Magnetic Resonance (MAS–NMR) spectroscopies [1], [2], [3], [4], [5], [6], [7], [8], [9], [10] and [11]. These studies revealed the existence of non-apatitic environments of the mineral ions especially phosphates and carbonates, which could be easily observed by these techniques. These non-apatitic locations do not seem to correspond to those found in well-crystallized

calcium phosphates such as DiCalcium Phosphate Dihydrate (DCPD) or OctaCalcium Phosphate (OCP) although they share some common characteristics [2]. The non-apatitic ionic environments are believed to correspond to ions in a hydrated layer on the surface of the mineral crystals. Spectroscopic techniques (FTIR, NMR) have shown that the HPO_4^{2-} and CO_3^{2-} ions in non-apatitic environments could be rapidly and reversibly exchanged with ions of the solution without altering the main characteristics of the nanocrystals such as crystal size, shape or even the unit-cell dimensions of the apatite lattice or the position of the vibrational bands of apatitic groups [12]. Recent studies have shown that calcium ions of PCA could also participate to these rapid ion exchange reactions [13] and [14]. However, unlike for phosphate and carbonate ions any direct spectroscopic evidence for a discrimination of calcium environment in apatitic compounds did not exist. Recently, a study of bone crystals by X-ray emission spectroscopy suggested the existence of additional coordination types of P and Ca polyhedra in PCA structure [15].

The present study aims to accurately determine the spectroscopic characteristics of calcium ions in several apatitic and non-apatitic compounds of biological interest and to connect these observations with data already obtained on the non-apatitic environments of phosphate ions in poorly crystalline apatites analogous to bone mineral.

2. Materials and methods

The main calcium phosphates samples were prepared according to previously published methods: DiCalcium Phosphate Dihydrate (DCPD) [2], Anhydrous DiCalcium Phosphate (DCPA) [2], OctaCalcium Phosphate (OCP) [2], Amorphous Calcium Phosphate (ACP) [16], alpha and beta TriCalcium Phosphate (α- or β-TCP) [16], and stoichiometric HydroxyApatite (s-HA) [17]. All samples were checked by X-ray diffraction and FTIR spectroscopy and furnished the expected patterns. The poorly crystalline apatites were prepared by double decomposition between a calcium nitrate and an ammonium phosphate solution [18]. Maturation was carried out in the mother solution for chosen periods of time before filtration, washing and lyophilization. The chemical composition of the samples was obtained by standard analysis procedures [2]. The amount of non-apatitic environments of phosphate groups was determined by FTIR spectroscopy and decomposition of the ν_4 PO_4 band using Grams 5 (Galactic, Salem NH). The phosphate domain was decomposed into 7 components in the domain of interest, according to previous studies [2] and [13].

For those experiments fine powders of the different reference compounds, previously ground to a smooth powder in an agate mortar and regular in size, were homogeneously layered between two 4 μm thick ultralene foils (SPEX-CERTIPREP, NJ). The thickness and homogeneity of the samples were optimized to obtain a good signal to noise ratio in transmission, i.e. introducing around 80% absorption.

The study was carried out at the X-ray microscopy beamline ID21 at the ESRF (European Synchrotron Radiation Facility) in Grenoble (France). An energy range between 2000 and 7000 eV is available at the ID21 beamline, which gives access in particular to the K-edge of calcium at 4038.5 eV to perform X-ray Absorption Near Edge Structure (XANES) spectroscopy experiments. The energy scan was ensured by a fixed exit double crystal Si(111) monochromator, located upstream the microscope, which offers an energy resolution of $\Delta E/E = 10^{-4}$ necessary to resolve the XANES structures. The XANES spectra were obtained in transmission mode, with a Si photodiode mounted downstream the sample, in a non-focused mode, the size of the beam being determined by a 200 μm pinhole. The incident beam intensity was monitored using a photodiode with a central hole, inserted in the beam and measuring the fluorescence signal from a thin 1.5 μm aluminum foil covering it. This so-called I_0 measurement is essential for normalizing the transmitted beam signal.

Experiments were performed at room temperature and atmospheric pressure. Spectra were collected in an energy range between 4020 and 4140 eV, with energy steps of 0.3 eV and 1 sec dwell time per point. The objective of this first experiment was to collect XANES reference spectra to have some background to perform spatially resolved XANES (at the micrometer scale) on biological sample; unfortunately, the EXAFS domain is not available on the ID21 beamline with the spatially resolved configuration so this domain was not considered on reference sample in a first step.

Data analysis was carried out following standard procedures [19]: the energy origin E_0 was taken at the inflection point of the absorption edge and, after subtracting the background contribution for lower energy edges, based on a polynomial fit of the preedge region, the postedge absorption was normalized to unity using XANES dactyloscope [20]. Complementary data processings (spectral subtraction, derivative spectra) were performed with XOP 2.0 [21] and Grams 5 (Galactic, Salem NH) as developed in Experimental results. The position of the narrow structures was determined from the second derivative of the spectra and the position of the broad structures directly from absorption spectra.

2.1. Structural characteristics of calcium phosphates

Apatites form a vast family of ionocovalent compounds represented by the general chemical formula: $Me_{10}(XO_4)_6Y_2$ where Me is a bivalent ion, XO_4 a trivalent ion and Y a monovalent ion. The structure is hexagonal (space group $P6_3/m$).

For example, hydroxyapatite can be described as a hexagonal stack of PO_4^{3-} groups creating two kinds of tunnel parallel to the c axis [22] and [23]. The first kind of tunnel, coinciding with the ternary axis of the structure, is occupied by Ca^{2+} noted as Ca(I) ions whereas the second one, which is lined by oxygen and other calcium ions, noted Ca(II), is occupied by OH^- ions (Fig. 1). The diameter of such tunnels (3 Å in s-HA) gives apatites ion exchanger properties but only at high temperatures, and it can also act as a host to small molecules [22] and [24]. Such a structure induces a wide range of distances between the calcium and the oxygen atoms and leads to an extremely complicated XAS spectrum.

Fig. 1. Projection on the (001) plane of the hydroxyapatite structure. The two Ca^{2+} triangles lining the "tunnels" of the structure are located at *z* 1/4 and *z* 3/4. OH^- ions are slightly under or above the triangles.

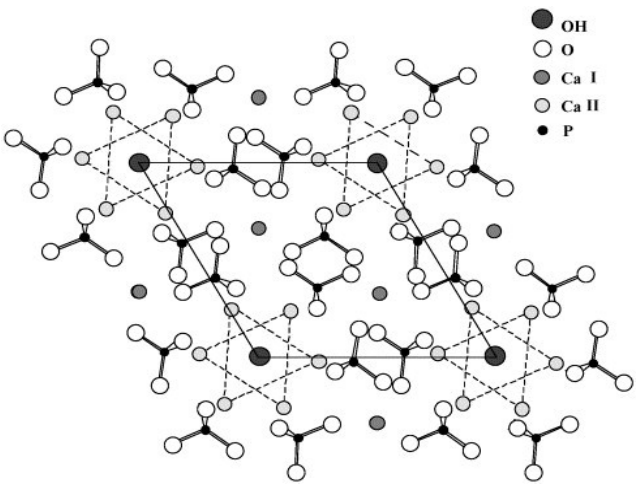

As another example, OCP structure can be described as lamellar with an assembly of dense sheets, corresponding to half the apatitic cell, and hydrated sheets, corresponding to the chemical composition of DCPD (Fig. 2). The "apatite" layer consists of alternating sheets of phosphate ions interspersed with Ca^{2+} ions; and the hydrated layer consists of more widely spaced phosphate and Ca^{2+} ions with a slightly variable number of water molecules between them. Six of the Ca^{2+} ions and two of the phosphate ions are in the "apatite" sheet. The other two Ca^{2+} ions and one phosphate ion are in the "hydrated" sheet. The remaining three phosphate ions lie at the junction of the "hydrated" and "apatite" sheets.

Fig. 2. Projection on the (001) plane of the octacalcium phosphate (OCP) structure. The "apatitic" domain corresponds to the upper lozenge, analogous to the apatite structure (see Fig. 1) and the lower quadrilateral to the OCP structure. Water molecules: only the oxygen atoms of the water in the hydrated layer are represented.

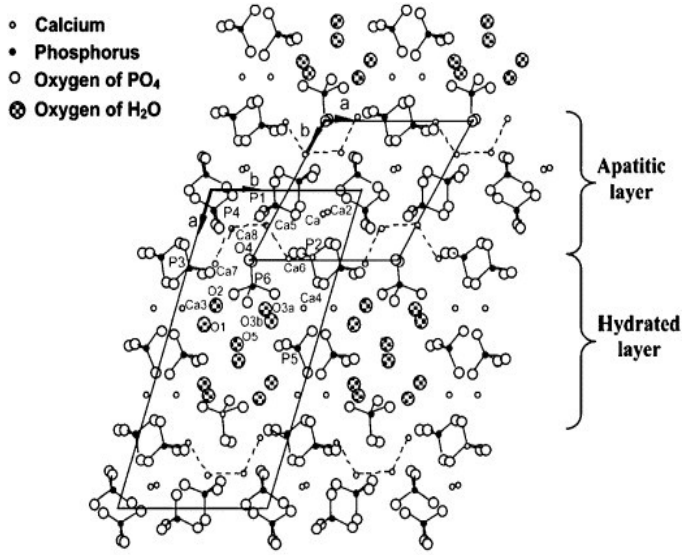

Finally, DCPD structure contains columns of alternating Ca^{2+} and HPO_4^{2-} ions. These columns are joined together to form corrugated sheets which are linked together by water molecules.

3. Experimental results

The data obtained for several calcium phosphates of biological interest are reported in Fig. 3 and Fig. 4A.

Fig. 3. XANES spectra at the Ca K-edge of different non-apatitic calcium phosphate compounds. (DCPD: DiCalcium Phosphate Dihydrate, DCPA: Anhydrous DiCalcium Phosphate, OCP: OctaCalcium Phosphate, ACP: Amorphous Calcium Phosphate, β-TCP: Beta Tri-Calcium Phosphate, α-TCP: alpha Tri-Calcium Phosphate).

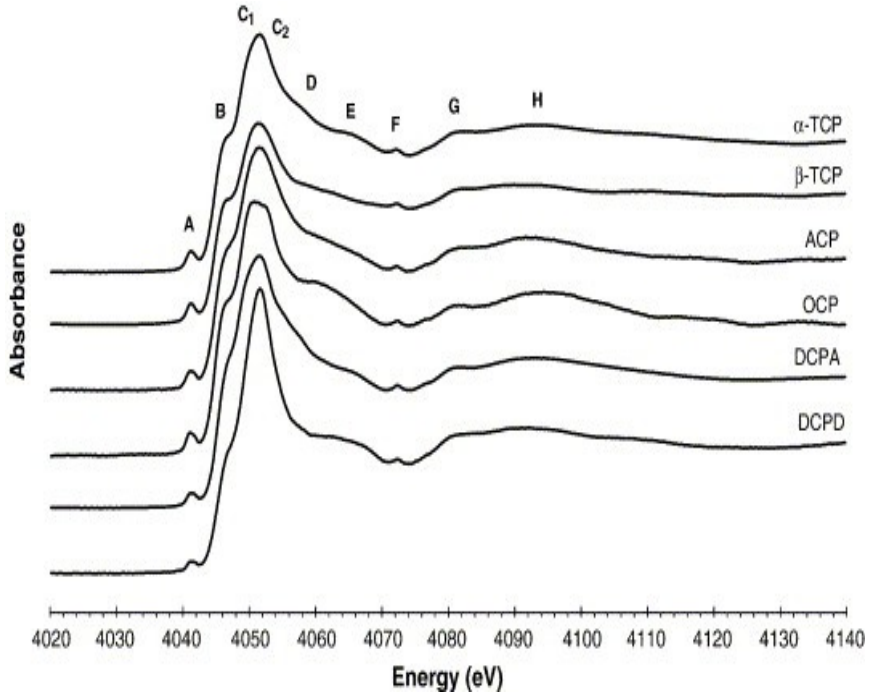

Fig. 4. (A) XANES spectra at the Ca K-edge of apatitic calcium phosphates. s-HA: Stoichiometric HydroxyApatite, PCA: Poorly Crystalline Apatite at different maturation stages (0: without maturation, 3d: 3 days, 16m: 16 months). (B) Derivatives of the XANES spectra in the domain 4040 – 4140 eV. s-HA: Stoichiometric hydroxyapatite, OCP: OctaCalcium Phosphate, PCA: Poorly Crystalline Apatite at different maturation stages (0: without maturation, 2h: 2 hours, 1d: 1 day, 3d: 3 days, 16m: 16 months). (C) XANES spectra of apatitic calcium phosphates in the domain 4070–4120 eV. s-HA: Stoichiometric HydroxyApatite, PCA: Poorly Crystalline Apatite at different maturation stages (0: without maturation, 1d: 1 day, 3d: 3 days, 1m: 1 month, 16m: 16 months).

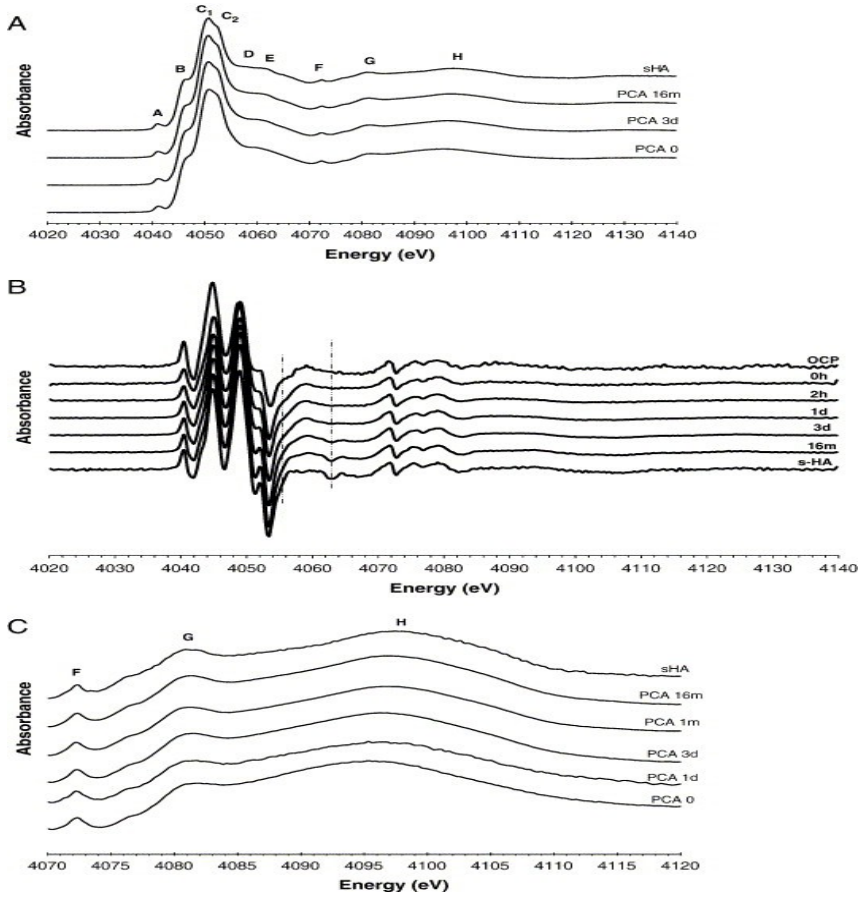

Within the energy region of interest, about 50 eV above the edge, it is possible to identify up to eight XANES structures, labelled from A to H as energy increases.

All the experimental spectra of the standard compounds (Fig. 3) show a small feature (labelled A) at the preedge. In general, spectral features a few eV (10 eV) before the edge threshold are due to electronic transitions to unoccupied states near the Fermi level and are sensitive to the spatial and electronic details of the potential. So the preedge, whose energy position (A: 4042 eV) remains the same but whose intensity varies, suggests that effective charge and site symmetry of the Ca ion changes across the compounds. This feature is commonly attributed to the 1s energy levels to bound 3d or O 2p molecular orbital [25]. As the transitions are here discrete, with broadening due to core-hole lifetime, this prepeak can be attributed to a 1s→3d transition, being dipole forbidden ($\Delta l = 2$), resulting from mixing of unoccupied d final states with p-character final states. The intensity of 1s→3d transition in first row transition metals will be stronger in compounds that are distorted from centrosymmetry [25].

As the energy increases, we find the most intense resonance of the spectra, called the white line, corresponding to the main 1s→np transition. The white line presents a characteristic three-peaks structure composed of a shoulder-like structure (labelled B, 4047 eV) at the low energy side that remains unaltered across the series and assigned to the 1s→4s transition, and a principal peak corresponding to the allowed 1s→4p transition, which is composed of two peaks (C_1 and C_2), whose relative intensities should depend of the type of Ca involved (type I or II) and may be linked to the concept of stoichiometry and non-stoichiometry in our samples [26]. As for D (4058.6 eV), it corresponds to transition to unoccupied states mainly from 5s states [27]. In addition, further XANES structures (labelled from E to H) are resolved at higher energies for all the compounds and are mainly due to multiple scattering contributions.

To sum up, the spectra of the standards show common features, present in each and all second derivative of the samples' spectra, but also very distinct and specific structures, (relative to the

considered spectrum) for each calcium salts. Common features consist in: the preedge peak labelled A at 4042 eV, a shoulder B at 4047 eV, a shoulder D at 4058.6 eV (more or less seen but always present in the second derivative spectrum) and a narrow distinct feature F at 4073.4 eV. All these sharp features suggest a transition with well-defined energy levels that seems to be invariant whatever the calcium phosphate compound considered. Another feature is present on all spectra, a broad structure G at 4081.5 eV, the position of which seems also independent of the phosphate salt considered. In addition to these common features, each salt presents specific structures related to transitions sensitive to the environment.

DiCalcium Phosphate Dihydrate (DCPD, $CaHPO_4$, $2H_2O$) is characterized by a unique white line at 4052.6 eV and broad structures centered at about 4064, 4093 and 4107 eV. The spectrum of anhydrous dicalcium phosphate (DCPA, $CaHPO_4$) is more complex with several shoulders (4050 and 4056.3 eV) on the white line located at 4052.9 eV. A very broad feature is then observed at 4094 eV.

Octacalcium phosphate (OCP, $Ca_8(PO_4)_4(HPO_4)_2$, $5H_2O$): in addition to the common features, OCP shows a split white line like all apatitic samples (4050.7 and 4053.8 eV). Broad structures are at 4096, 4117 and 4134 eV.

A rather broad white line at 4052.4 eV characterizes the amorphous calcium phosphate (ACP). Broad structures are also apparent at 4064, 4094, 4117 and 4135 eV.

The crystalline β-tricalcium phosphate (β-TCP, $Ca_3(PO_4)_2$) provides a spectrum with a wide white line at 4052 eV and a wide shoulder at 4063 eV. Broad structures are also present at 4092 and 4110 eV. The spectra of α-tricalcium phosphate appear more complex with a distorted white line showing two components at 4050.2, 4052.9 eV and broader structures at 4066, 4094 and 4111 eV.

The spectrum of stoichiometric hydroxyapatite (s-HA, $Ca_{10}(PO_4)_6(OH)_2$, Fig. 4A) is characterized by a split white line with two components at 4051.4 and 4053.5 eV and shoulders at 4059, 4063, and 4067 eV, plus wide lines at 4099 and 4133 eV.

The spectra of poorly crystalline apatites at different maturation stages exhibit very similar features with a split white line (C_1, C_2; Fig. 4A). The preedge energy position and intensity seem to be independent of the maturation state of our PCA, suggesting that both the effective charge and the site symmetry of the Ca atom remain unaltered across the series.

But as the maturation time increases a faint narrowing of the white line is observed. There is also a modification of the curvature between points E and F. The changes are easily seen by considering the derivatives of the different spectra (Fig. 4B). With maturation time, the structures at 4056 and 4063 eV became more pronounced. It is important to notice that these structures seem to evolve from structures close to those present in the OCP spectrum to those of the s-HA spectrum. The most interesting feature however is a progressive displacement of the broad line maximum (H) from 4096.2 to 4098.1 eV during maturation (Fig. 4C). The difference spectra obtained by subtraction of the spectra of immature precipitate from that of matured samples indicate in fact the existence of an additional structure at 4092.5 eV in the most immature samples, which progressively decreases as the maturation time of the precipitate increases. This line is also observed with an appreciable intensity in OCP, brushite and amorphous Ca–P but it is completely vanished in stoichiometric hydroxyapatite.

This progressive displacement of the broad peak maximum towards higher energy can be related in a first approximation, without entering in details in the EXAFS theory such as second neighbors of the calcium ion and multiple scattering effect, to a modification of the length of the Ca–O bond, which becomes smaller as the maturation time increases [15], and the narrowing of the white line can be related to a progressive organization of the structure of our compounds.

Indeed, the position of the broad line maximum was found to vary considerably as a function of the maturation stage of the mineral.

4. Discussion

Previous observations have indicated that the XAS spectra at the calcium K-edge are very sensitive to the environment of the ion [26], [27] and [28]. In well-crystallized phases the observed spectra could be accurately reconstructed by considering the atoms in a 7 Å diameter sphere around the calcium atom. The splitting of the main white line in all apatitic samples has been assigned to the existence of two calcium sites with different coordination spheres [29]. It is remarkable that the same structure is observed for OCP, which is often described as a layered compound formed of a succession of apatite and hydrated layers but with 8 different environments of the calcium ions [30] and [31]. In all other cases, including the amorphous phase, the white line shows a unique structure. XANES allows then distinguishing between different types of calcium environments in several Ca–P structures of biological interest. The main observation is that the XANES Ca spectra of PCA are not identical to those of stoichiometric apatites confirming thus previous observations made by different spectroscopic techniques that mineral ions exhibit different environments in apatites.

Moreover, the sensitivity of the technique allows also the detection of faint variations of the environment of calcium ions in PCA during aging of the precipitate in solution. Although the XAS Ca spectrum of PCA just after precipitation appears very close to that of OCP, they differ essentially by the splitting of the white line, larger in OCP, but the other structures are superimposable. It shall be noted also that the additional structure (H) observed at early maturational stages at 4092.5 eV, is at the same position in the DCPD spectrum. Such analogies were also noticed for phosphate group's environments by other spectroscopic techniques [32] and [33]. It has been suggested that a progressive evolution from OCP to apatite can occur by a topotactic reaction corresponding to the elimination of the hydrated layer [34]. But it is important to note that the spectral characteristics of the non apatitic environments, which are responsible for the high reactivity of nanocrystalline apatites (including maturation), revealed by FTIR and NMR [35] cannot be assigned to any of the well crystallized calcium phosphate phases.

Like in previous spectroscopic studies, the XAS spectra do not allow a precise identification of the environments of the mineral ions in PCA with those existing in well-crystallized compounds.

The variations of the Ca environments observed by XAS were compared to other parameters relative to the maturation of calcium phosphates.

The evolution of the intensity of the broad structures maximum from 4096.2 to 4098.1 eV during maturation seems related to the variations of different indicators of maturation. Thus the increase of relative intensity of this structure with time is well correlated to the evolution of the Ca/P ratio (chemically measured) and seems also inversely related with the amount of labile HPO_4^{2-} determined by FTIR spectroscopy (Fig. 5A,B). This displacement (shift of the broad structure to higher energy) is also the immediate criteria to represent the modification of the Ca–O bond length, which is found to become smaller as maturation time increases. The narrowing of the white line constitutes another indication that our PCA are evolving to stoichiometry, as it confirms that the Ca–O bond length is decreasing and that the PCA structure is better organized with time. The study of the derivatives of the different spectra indicates as well an increase of the stoichiometry through maturation time as the structures are getting closer to that present in the s-HA spectrum. Other correlations with other indicators of maturation such as crystal size or strains may also be observed and few authors have made the analogous observations [36]. Although these correlated variations do not indicate that these parameters are strictly connected, the similarity of chemical behavior between labile HPO_4^{2-} and labile Ca^{2+} ions suggests however

that these ions share the same environments and might be connected.

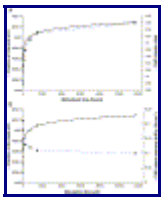

Display Full Size version of this image (49K)

Fig. 5. (A) Correlation between the position of the XANES broad structure (H) from 4096.2 to 4098.1 eV and the Ca/P ratio (chemically measured) during maturation of PCA. The displacement of this broad structure to higher energy might be related to the physical parameter of the diminution of the Ca–O bond length. (B) Correlation between the position of the XANES broad structure from 4096.2 to 4098.1 eV and the labile HPO_4^{2-} content determined from FTIR spectra.

5. Conclusion

The data obtained by XAS confirm the existence in immature non-stoichiometric apatites of different types of calcium environments and especially of non-apatitic environments of calcium ions. As several biological properties of bone (protein attachment, ion exchange and homeostasis) are related to these surface environments, it seems important to have a possibility to reach the highly reactive calcium sites of bone and other biological samples involving poorly crystalline apatites by a direct spectroscopic method. The XAS technique, combined with the sub micron spatial resolution available with the ID21 Scanning X-ray Microscope, should allow an in situ mapping of the maturation stage of PCA in bone or other tissues from the analysis of calcium environments. To try to fully characterize the environment of the calcium ion in our biological apatites, the EXAFS part of the X-ray absorption spectra seems interesting to investigate. It should allow us to probe very precisely and semi quantitatively the precise atomic environment of our calcium atom by giving access to the interatomic distances, the coordination number and the relative displacements in our calcium phosphates. Such measurements are in progress.

Acknowledgements

The authors are very grateful to R. Baker, G. Berruyer, F. Demarcq, F. Thurel for their technical assistance. The experiments were supported by ESRF in the framework of CH-1266 proposal and were carried out at the ID21 X-ray Microscopy Beamline. We thank ESRF for providing beam time.

References

C. Rey, B. Collins, T. Goehl, R.I. Dickson and M.J. Glimcher, The carbonate environment in bone mineral. A resolution enhanced Fourier transform infrared spectroscopy study, *Calcif. Tissue Int.* 45 (1989), pp. 157–164.

C. Rey, B. Collins, M. Shimizu and M.J. Glimcher, Resolution enhanced Fourier transform infrared spectroscopic study of the environment of phosphate ion in the early deposits of a solid phase of calcium phosphate in bone and enamel and their evolution with age: I. Investigation in the ν_4 PO_4 domain, *Calcif. Tissue Int.* 46 (1990), pp. 384–394.

S.J. Gadaleta, E.P. Paschalis, F. Betts, R. Mendelsohn and A.L. Boskey, Fourier transform infrared spectroscopy of the solution-mediated conversion of amorphous calcium phosphate to

hydroxyapatite: new correlations between X-ray diffraction and infrared data, *Calcif. Tissue Int.* 58 (1996), pp. 9–16.

L.M. Miller, V. Vairavamurthy, M.R. Chance, R. Mendelsohn, E.P. Paschalis, F. Betts and A.L. Boskey, In situ analysis of mineral content and crystallinity in bone using infrared micro-spectroscopy of the ν_4 PO_4^{3-} vibration, *Biochim. Biophys. Acta* 1527 (2001) (1–2), pp. 11–19. S. Bohic, D. Heymann, J.A. Pouezat, O. Gauthier and G. Daculsi, Transmission FT-IR microspectroscopy of mineral phases in calcified tissues, *C.R. Acad. Sci. III-VIE* 321 (1998), pp. 865–876. Cited By in Scopus (0)

D. Magne, P. Weiss, J.M. Bouler, O. Labroux and G. Daculsi, Study of the maturation of the organic (type I collagen) and mineral (nonstoichiometric apatite) constituents of a calcified tissue (dentin) as a function of location: a Fourier transform infrared microspectroscopic investigation, *J. Bone Miner. Res.* 16 (2001), pp. 750–757. G. Sauer, W.B. Zunic, J.R. Durig and R.E. Wuthier, Fourier transform Raman spectroscopy of synthetic and biological calcium phosphates, *Calcif. Tissue Int.* 54 (1994), pp. 414–420.

K. Beshah, C. Rey, M.J. Glimcher, M. Shimizu and R.G. Griffin, Solid state carbon-13 and proton NMR studies of carbonate containing calcium phosphates and enamel, *J. Solid State Chem.* 84 (1990), pp. 71–81.

Y. Wu, M.J. Glimcher, C. Rey and J. Ackerman, A unique protonated phosphate group in bone mineral not present in synthetic calcium phosphates, *J. Mol. Biol.* 244 (1994), pp. 423–435.

Y. Wu, J. Ackerman, E. Stawitch, H.-M. Kim, C. Rey, A. Barroug and M.J. Glimcher, Nuclear magnetic resonance spin–spin relaxation of the crystals of bone, dental enamel and synthetic hydroxyapatites, *J. Bone Miner. Res.* 17 (2002), pp. 472–480.

Y. Wu, J.L. Ackerman, E.S. Strawich, C. Rey, H.-M. Kim and M.J. Glimcher, Phosphate ions in bone: identification of a calcium–organic phosphate complex by ^{31}P solid-state NMR spectroscopy at early stages of mineralization, *Calcif. Tissue Int.* 725 (2003), pp. 610–626.

C. Rey, A. Hina, A. Tofighi and M.J. Glimcher, Maturation of poorly crystalline apatites: chemical and structural aspects in vivo and in vitro, *Cells Mater.* 5 (1995) (4), pp. 345–356.

D. Eichert, Etude de la réactivité de surface d'apatites de synthèse nanocristallines, Thèse INPT, Toulouse, 2001.

S. Cazalbou, Echanges cationiques impliquant des apatites analogues au minéral osseux, Thèse INPT, Toulouse, 2000.

J. Rakovan and R.J. Reeder, Intracrystalline rare earth element distributions in apatite: surface structural influences on incorporation during growth, *Geochim. Cosmochim. Acta* 60 22 (1996), pp. 4435–4445.

S. Somrani, C. Rey and M. Jemal, Thermal evolution of amorphous tri-calcium phosphate, *J. Mater. Chem.* 13 (2003), pp. 888–892.

J. Arends, J. Christoffersen, M.R. Christoffersen, H. Eckert, O. Fowler, J.C. Heughebaert, G.H. Nancollas, J.P. Yesinowski and S.J. Zawacki, A calcium hydroxyapatite precipitated from aqueous solution — an international multimethod analysis, *J. Cryst. Growth* 84 (1987), pp. 515–532.

C. Rey, V. Renugopalakrishnan, B. Collins and M.J. Glimcher, Fourier transform infrared spectroscopy study of the carbonate ions in bone mineral during aging, *Calcif. Tissue Int.* 49 (1991), pp. 251–258.

B. Lengeler and P. Eisenberger, Extended X-ray absorption fine structure analysis of interactomic

distance, coordination numbers and mean relative displacements in disordered alloys, *Phys. Rev. B* 21 (1980), pp. 4507–4520.

K. V. Klementiev, "XANES dactyloscope 'for Windows', freeware: www.desy.de/~klmn/xanda.html".

M. Sanchez del Rio and R.J. Dejus, *XOP: Recent Developments* vol. 2448, SPIE (1998), pp. 340–345.

J.C. Elliott, Structure and Chemistry of the Apatites and Other Calcium Orthophosphate, Elsevier, Amsterdam, The Netherlands (1994).

M.I. Kay, R.A. Young and A.S. Posner, Crystal structure of hydroxyapatite, *Nature* 204 (1964), pp. 1050–1052.

Some aspects of crystal structural modeling of biological apatites, *Colloq. Int. CNRS* vol. 230, CNRS, Paris (1973), pp. 21–40.

B. Ravel and E.A. Stern, Local disorder and near edge structure in titanate perovskites, *Phys., B Condens. Matter* 208–209 (1995), pp. 316–318.

K. Asokan, J.C. Jan, J.W. Chiou, W.F. Pong, P.K. Tseng and I.N. Lin, X-ray absorption spectroscopy studies of $Ba_{1-x}Ca_xTiO_3$, *J. Synchrotron Radiat.* 8 (2001), pp. 839–841. J. Chaboy and S. Quartieri, X-ray absorption at the Ca K edge in natural garnet solid solutions: a full-multiple scattering investigation, *Phys. Rev. B* 52 (1995), pp. 6349–6357. S.C. Liou, S.Y. Chen, H.Y. Lee and J.S. Bow, Structural characterization of nano-sized calcium deficient apatite powders, *Biomaterials* 25 (2004), pp. 189–196.

A.P. Shpak, V.L. Karbovskii and V.V. Trachevskii, Peculiarities of the electronic structure of the ultra disperse calcium hydroxyapatite, *J. Electron Spectrosc. Relat. Phenom.* 88–91 (1998), pp. 973–976.

W.E. Brown, M. Mathew and M.S. Tung, Crystal chemistry of OCP, *Prog. Cryst. Growth Charact.* 4 (1981), pp. 59–87.

M. Mathew, W.E. Brown, L.W. Schroeder and B. Dickens, Crystal structure of octacalcium bis(hydrogenphosphate) tetrakis (phosphate) pentahydrate, $Ca_8(HPO_4)_2(PO_4)_4, 5H_2O$, *J. Crystallogr. Spectrosc. Res.* 18 (1998), pp. 235–250.

G. Penel, G. Leroy, C. Rey and E.F. Brès, Microraman spectral study of carbonated apatites, enamel, dentine and bone, *Calcif. Tissue Int.* 63 (1998), pp. 475–481.

D. Eichert, results to be published.

W. Brown, L. Schroeder and J. Ferris, Interlayering of crystalline octacalcium phosphate and hydroxyapatite, *J. Phys. Chem.* 83 (1979), pp. 1385–1388.

D. Eichert, H. Sfihi, C. Combes and C. Rey, Specific characteristics of wet nanocrystalline apatite. Consequences on biomaterials and bone tissue, *Trans. Tech. Publications* 256 (2004), pp. 927–930.

A. Boskey, N. Pleshko, S.B. Doty and R. Mendelsohn, Application of Fourier transform infrared (FT-IR) microscopy to the study of mineralization in bone and cartilage, *Cells Mater.* 2 (1992), pp. 209–220.

Corresponding author. Tel.: + 33 (0)4 76 88 28 86; fax: +33 (0)4 76 88 27 85.

Original text : Elsevier.com